PROCEEDINGS OF SCIENCE

Measurements of HF-tagged jet substructure and energy-energy correlators with ALICE

Marianna Mazzilli for the ALICE Collaboration[a,*]

[a] *University of Houston*
Houston, USA

E-mail: marianna.mazzilli@cern.ch

Properties of partonic fragmentation in quantum chromodynamics (QCD) depend on parton flavours in $1 \rightarrow 2$ splitting processes in parton showers due to the different Casimir factors of quarks and gluons, and to the different masses of light- and heavy-flavour quarks. Heavy-flavour jets provide a unique experimental tool to probe these flavour dependencies. They represent an enhanced sample of jets originating from quarks and, at low and intermediate transverse momenta, they exhibit sensitivity to mass-related effects. This contribution presents a collection of jet substructure measurements, with a particular focus on the comparison of measurements of inclusive jets and D^0-meson tagged jets.

The European Physical Society Conference on High Energy Physics (EPS-HEP2023)
21-25 August 2023
Hamburg, Germany

*Speaker

PoS(EPS-HEP2023)262

1. Introduction

Jets are collimated bunches of hadrons that result from the fragmentation of partons following their scattering in the early stages of collisions. The specific characteristics of the resulting jets depend on the flavour of the initiating parton. Gluon-initiated jets, for example, are expected to exhibit a broader and softer fragmentation pattern compared to quark-initiated jets. This difference arises from their distinct Casimir colour factors. In the case of heavy-flavour jets, mass effects are also expected to arise from the dead-cone effect. This phenomenon restricts the emission phase space of a massive emitter within an angular region that is proportional to the emitter's mass [1]. Jet substructure measurements, based on the distribution of constituents within a jet, are able to probe specific regions of QCD radiation phase space for jet showers in vacuum. This powerful capability provides new opportunities to study fragmentation patterns of parton showers in vacuum and the dynamics of jet quenching in heavy-ion collisions, probing our current understating of perturbative QCD (pQCD). Jet substructure can also be used to study non-perturbative effects including hadronisation. Different jet clustering algorithms can be applied to group the final-state particles originating from the scattered parton. By utilising a set of substructure observables alongside fully reconstructed heavy-flavour hadrons, we can effectively characterise the influence of mass and colour-charge effects in the fragmentation process.

2. Accessing the charm splitting function

The usage of an iterative reclustering technique, the Cambridge–Aachen (C/A) algorithm [2], on jets reconstructed with the anti-k_{T} algorithm [3] gives access to individual splittings inside a jet under the assumption of angular ordering. In particular, splittings are tagged using the Soft Drop grooming condition [4], which reveals perturbative splittings within the jet. At each declustering step the splitting is tested against the Soft Drop condition, as given by:

$$z \equiv \frac{\min(p_{\mathrm{T},1}, p_{\mathrm{T},2})}{p_{\mathrm{T},1} + p_{\mathrm{T},2}} > z_{\mathrm{cut}} \left(\frac{\Delta R_{1,2}}{R}\right)^{\beta} \tag{1}$$

where $p_{\mathrm{T},1}$ and $p_{\mathrm{T},2}$ are the transverse momenta of the leading and subleading prongs of the splitting, respectively, and R is the jet resolution parameter. The grooming behaviour is defined by parameters z_{cut} (with $z_{\mathrm{cut}} = 0.1$) and β (with $\beta = 0$) which control the interplay between the shared momentum fraction z and the aperture angle between the prongs $\Delta R_{1,2}$. The groomed-jet substructure is often characterised by the groomed momentum fraction z_g, defined as the values of z corresponding to the first hard splitting fulfilling the soft-drop condition [7]. The z_g distributions in Fig. 1 shows that charm-tagged jets have significantly fewer symmetric splittings (large z_g values) compared to inclusive jets, as a consequence of the larger colour charge of gluons. Both the PYTHIA 8 [5] and POWHEG [6] + PYTHIA 6 predictions for charm-quark jets describe the measurements within uncertainties [7].

3. Jet angularities with D^0-jets

Jet angularities represent a class of jet substructure observables which depends both on the p_{T} and on the angular distribution of constituents within the jet, individually weighted by the

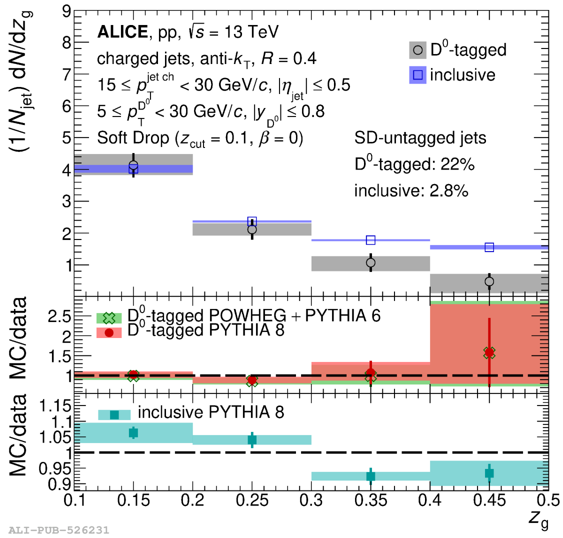

Figure 1: z_g distribution of prompt D^0-tagged jets compared to inclusive jets for $15 < p_{\mathrm{T,jet}} < 30$ GeV/c in pp collisions at $\sqrt{s} = 13$ TeV, normalised to the total number of jets. Model-to-data ratios are shown in the bottom panels for PYTHIA 8 and POWHEG + PYTHIA 6 simulations.

continuous parameters k and α, respectively:

$$\lambda_\alpha^k = \sum_{i \in jet} \left(\frac{p_{\mathrm{T,i}}}{p_{\mathrm{T,jet}}}\right)^k \left(\frac{\Delta R_{\mathrm{jet,i}}}{R}\right)^\alpha \quad (2)$$

where the first term of the product returns the jet $p_{\mathrm{T,i}}$ fraction carried by the constituent i and $\Delta R_{\mathrm{jet,i}}$ is the distance of the constituent i to the jet axis of radius R. For $\alpha > 0$ and $k = 1$ these observables are infrared and collinear (IRC) safe and, therefore, calculable with pQCD. The α parameter characterises the radiation pattern inside the jet and its variation tunes the sensitivity to mass and colour-charge effects. In Fig. 2 the angularity distributions with $\alpha = 1$ (left panel) and $\alpha = 3$ (right panel) is compared for D^0-tagged jets and semi-inclusive jets. For $\alpha = 1$, D^0-tagged jets are most different at low $\lambda_{\alpha=1}$ ($\lambda_{\alpha=1} < 0.2$), indicating that in this region D^0-tagged jets emissions are more concentrated than semi-inclusive ones. For larger α, where a larger sensitivity to the colour charge effect is expected, the shape of the two angularity distributions is more similar. In both cases, PYTHIA 8 [5] predictions reproduce the shape of the data, though some tension is observed particularly for the inclusive measurements.

4. D^0 tagged jet-axis differences

A novel jet-substructure observable consisting in the angle between two definitions of the axis of a jet:

$$\Delta R_{\mathrm{axis}} \equiv \sqrt{(y_2 - y_1)^2 + (\varphi_2 - \varphi_1)^2} \quad (3)$$

has been studied [8]. The different definition used for the jet-axis determination allows us to differentially probe the sensitivity to the soft radiation in the parton shower. The "standard (STD)"

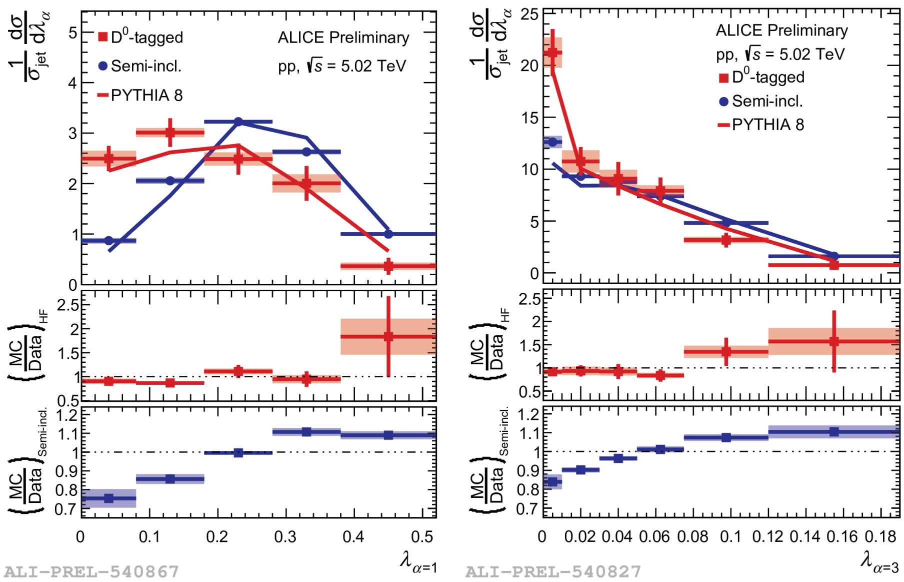

Figure 2: Angularity distributions with α = 1 (left panel) and α = 3 (right panel) for D^0-tagged jets (red points) and semi-inclusive jets (blue points). The data are compared with PYTHIA 8 expectations reported with solid curves.

axis is determined by clustering the jet constituents with the anti-$k_{\rm T}$ algorithm and the E recombination scheme. The "groomed" axis definition is less sensitive to the non-perturbative effects as it systematically removes the soft wide-angle radiation in the jet and determines the axis of the anti-$k_{\rm T}$ jet (with E recombination scheme), clustering only the constituents that remain after grooming. A third definition of the jet axis consists in reclustering the jet with the angular-ordered C/A algorithm [2]. Subsequently, the constituents are recombined with the Winner-Takes-All (WTA) transverse-momentum recombination scheme [9] which tends to align the jet axis with the most energetic particle of the jet. As a result, the WTA resulting axis is insensitive to soft radiation. A preliminary study of the difference of the jet axis with the standard algorithm and D^0 directions shows that the charm meson tends to be collinear with the jet axis. The $\Delta R_{\rm STD-D^0}$ distribution is reported in the left panel of Fig. 3 and it is in agreement with PYTHIA 8 predictions. On the right panel, the $\Delta R_{\rm WTA-D^0}$ distributions obtained with PYTHIA 8 confirm that the WTA algorithm better aligns the jet axis with the hardest prong (D^0 mesons). Comparing $\Delta R_{\rm WTA-D^0}$ distribution with $\Delta R_{\rm WTA-STD}$ of inclusive jets, reported in Ref. [8], D^0 mesons are more collinear with the jet axis than the hardest prong of inclusive jets, pointing towards a narrowing of the heavy-flavour jets with respect to inclusive jets. These studies serve as baseline for future measurements of heavy-flavour jet $\Delta R_{\rm axis}$ in Pb–Pb collisions, where crucial insights on the in-medium energy loss mechanism can be obtained.

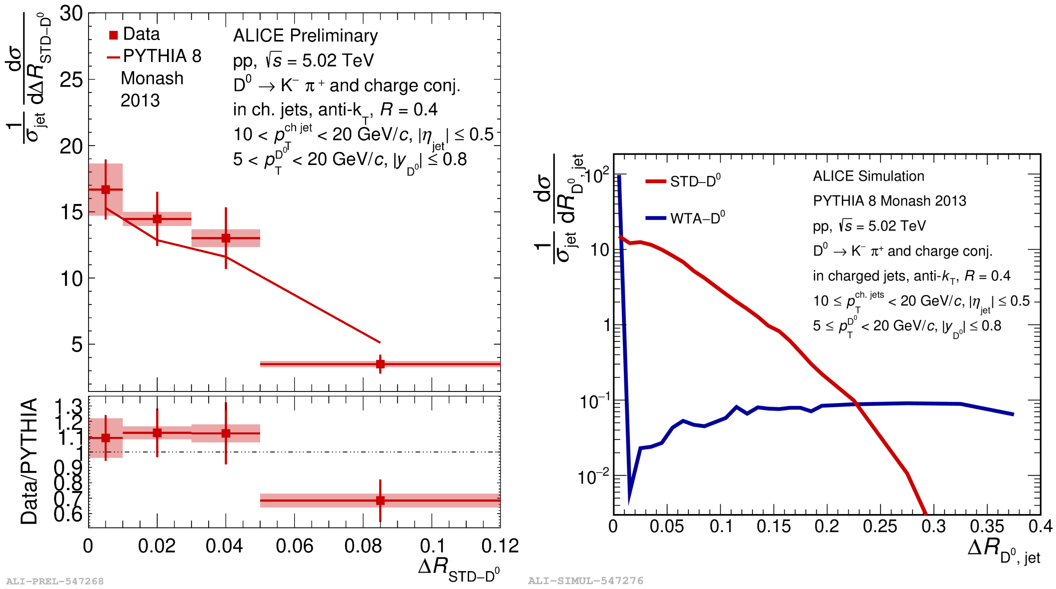

Figure 3: Left: $\Delta R_{\rm STD-D^0}$ distribution in pp collisions at $\sqrt{s}$ = 5.02 TeV compared with PYTHIA 8 predictions. Right: comparison of PYTHIA 8 predictions for $\Delta R_{\rm STD-D^0}$ and $\Delta R_{\rm WTA-D^0}$ distributions.

5. Energy-energy correlator

Recently, a novel jet substructure observable, energy-energy correlators (EEC), has been proposed to study the angular structure of energy flow within jets. It is defined as:

$$\frac{d\sigma_{\rm EEC}}{dR_{\rm L}} = \sum_{i,j} \int d\sigma(R'_{\rm L}) \frac{p_{{\rm T},i}\, p_{{\rm T},j}}{p^2_{\rm T,jet}} \delta(R'_{\rm L} - R_{{\rm L},ij}) \tag{4}$$

where i, j correspond to a pair of jet tracks and $R_{\rm L} = \sqrt{\Delta\varphi^2_{ij} + \Delta\eta^2_{ij}}$ is the pair distance. The EEC quantifies the energy-weighted cross-section of particle pairs inside jets. The scaling behaviour of the EECs as a function of pair distance exposes a distinct separation of the perturbative from the non-perturbative regime and allows to probe parton-type dependent dynamics of jet formation and their confinement into hadrons. In Fig. 4, the normalised EEC cross section of inclusive jets in pp collisions at $\sqrt{s}$ = 5.02 TeV compared with next to leading-logarithmic (NLL) pQCD calculation [10] is reported. A good agreement between the pQCD calculation and data at the perturbative region (large $R_{\rm L}$) is observed. The EEC cross-section starts to deviate from the pQCD curve towards smaller $R_{\rm L}$, which is expected since the non-perturbative effects start to become more important. At very small $R_{\rm L}$ region, after the hadronization transition peak, the EEC cross section as a function of $R_{\rm L}$ follows a linear scaling behavior. In this non-perturbative region, hadrons are formed and freely moving. Hadron pairs with a smaller opening angle $R_{\rm L}$ occur less often because of the decrease of the phase space. Also the linear scaling description deviates from the data points towards the peak transition region.

As discussed in Ref. [11], the ratio between the EEC of heavy-flavour and light flavour jets represents a powerful tool to direct access the dead-cone effect with an observable that can be systematically computed in perturbation theory.

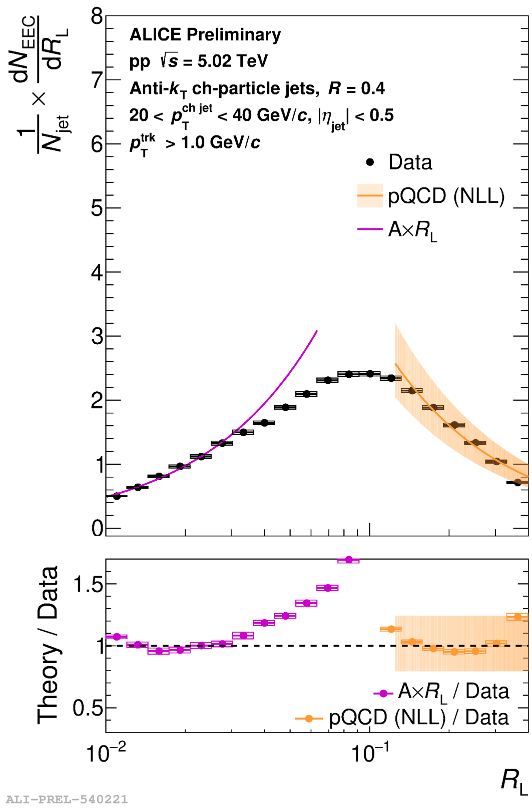

Figure 4: Comparison of the measured EEC distributions with NLL pQCD calculation [10] (orange curve) in the large angle region (perturbative region) and linear scaling function (purple curve) in the small angle region (non-perturbative region).

Regarding the non-perturbative region (hadronic region), the scaling behavior in this region corresponds to late formation/splitting time after hadrons formation time. Hadron pairs with a smaller opening angle R_L occur less often because of the decrease of the phase space.

6. Summary

The comparison of jet substructure measurements of fully reconstructed heavy-flavour hadrons and inclusive jets demonstrated the different evolution of the parton shower and indicated to be sensitive to flavour effects. The upgraded ALICE detector in the LHC Run 3 and Run 4 will extend these measurements to jets tagged with a fully reconstructed beauty meson and to more precise low-momenta measurement of charm jets, enabling the isolation of mass effects from the effects due to Casimir colour factors in pp and in Pb–Pb collisions.

References

[1] S. Acharya *et al.* [ALICE], Nature **605** (2022) no.7910, 440-446 [erratum: Nature **607** (2022) no.7920, E22] doi:10.1038/s41586-022-04572-w [arXiv:2106.05713 [nucl-ex]].

[2] Y. L. Dokshitzer, G. D. Leder, S. Moretti and B. R. Webber, JHEP **08** (1997), 001 doi:10.1088/1126-6708/1997/08/001 [arXiv:hep-ph/9707323 [hep-ph]].

[3] M. Cacciari, G. P. Salam and G. Soyez, JHEP **04** (2008), 063 doi:10.1088/1126-6708/2008/04/063 [arXiv:0802.1189 [hep-ph]].

[4] A. J. Larkoski, S. Marzani, G. Soyez and J. Thaler, JHEP **05** (2014), 146 doi:10.1007/JHEP05(2014)146 [arXiv:1402.2657 [hep-ph]].

[5] T. Sjöstrand, S. Ask, J. R. Christiansen, R. Corke, N. Desai, P. Ilten, S. Mrenna, S. Prestel, C. O. Rasmussen and P. Z. Skands, Comput. Phys. Commun. **191** (2015), 159-177 doi:10.1016/j.cpc.2015.01.024 [arXiv:1410.3012 [hep-ph]].

[6] S. Alioli, P. Nason, C. Oleari and E. Re, JHEP **06** (2010), 043 doi:10.1007/JHEP06(2010)043 [arXiv:1002.2581 [hep-ph]].

[7] [ALICE], [arXiv:2208.04857 [nucl-ex]].

[8] S. Acharya *et al.* [ALICE], JHEP **07** (2023), 201 doi:10.1007/JHEP07(2023)201 [arXiv:2211.08928 [nucl-ex]].

[9] D. Bertolini, T. Chan and J. Thaler, JHEP **04** (2014), 013 doi:10.1007/JHEP04(2014)013 [arXiv:1310.7584 [hep-ph]].

[10] K. Lee, B. Meçaj and I. Moult, [arXiv:2205.03414 [hep-ph]].

[11] E. Craft, K. Lee, B. Meçaj and I. Moult, [arXiv:2210.09311 [hep-ph]].

PoS(EPS-HEP2023)262